



## Level statistics and interactions in a two-dimensional quantum dot

SERGIO E. ULLOA

*Department of Physics and Astronomy and Condensed Matter and Surface Sciences Program,  
Ohio University, Athens, OH 45701-2979, U.S.A.*

DANIELA PFANNKUCHE

*Max-Planck Institut für Festkörperforschung, Heisenbergstr. 1, D-70569 Stuttgart, Germany*

(Received 20 June 1996)

---

The energy level structure of an interacting system of electrons is analysed. The model chosen describes electrons in a semiconductor quantum dot system, whose energy levels could be accessed via finite-bias transport experiments. We find that the normalized level spacing of the system exhibits significant departures from Poisson statistics, and that these are strongly dependent on magnetic field, and quantum numbers of the level sequence.

© 1997 Academic Press Limited

**Key words:** semiconductor, low-dimension, interactions, chaos.

---

### 1. Introduction

The dynamical behavior of classical systems that exhibit extreme sensitivity to initial conditions is known as *chaotic* or *non-integrable*. This behavior can appear because of a strong non-linear driving force, or even from relatively simple geometrical features of the region where particle motion is allowed. Perhaps one of the better known cases of the latter category is that of a particle moving in a two-dimensional region bounded by hard walls, a 'billiard'. If the shape of these walls is circular, the system is non-chaotic (and then classically integrable), while if there are departures from that shape, they would most probably produce chaotic behavior and cause the system to be 'K-flow' type [1].

A billiard formed with straight segments joining two semicircular halves (a 'stadium'), has received a great deal of attention. In particular, the stadium has been used as a prototype to illustrate the strong connection between the non-integrability of the system and the characteristics of the level spectrum in its quantum counterpart (a quantum particle moving inside this stadium geometry) [1–3]. The stadium has also been analysed for the appearance of 'scars' on the wavefunctions, showing strong enhancements along the points followed by classical periodic trajectories [4], and recently for the effects of applied magnetic fields on the level structure [5].

Detailed analysis of the fluctuations in the level structure of a quantum stadium, as well as in other systems, has shown that the integrability (or non-) of a classical system is accompanied by a characteristic distribution of levels. In the 'generic' integrable case, the nearest-neighbor level spacings are found to be well described by a Poisson distribution function. This is intuitively understood as coming from the arbitrary location of levels associated with different conserved quantities (and corresponding quantum numbers) [6]. On the other

hand, classical non-integrability corresponds to the appearance of non-conserved quantities, and the associated mixing and repulsion of nearby levels. This then yields a distribution of nearest-neighbor spacings peaked at a finite value, which is found to be well described by random matrix theory, as Wigner surmised for a gaussian ensemble [1, 3, 7].

In this paper, we study the effects of *particle interactions* on the level statistics of an otherwise integrable system. By considering a two-dimensional well with parabolic confinement (rather than the hard wall used in the billiards above), one can immediately solve the single-particle quantum problem as a set of harmonic oscillator levels. We show that when considering several particles and their mutual Coulomb interaction, the level structure undergoes strong deviations from both the integrable harmonic case, and the Poisson statistics of a ‘generic’ integrable system. This study is related to the level spectrum probed via tunneling experiments in semiconductor quantum dot systems, where finite-bias measurements explore the manifold of excited states in the system [8], and electronic correlations are believed to be important [9]. Transport and optical absorption experiments could therefore provide an interesting possible probe of the level structure we describe below. This is particularly relevant given that the characteristics of the level structure are strongly sensitive to applied magnetic fields accessible experimentally. Moreover, this study also complements theoretical work on the distribution of excited states in mesoscopic disordered metal particles, where the Wigner distribution has been proven to describe the level structure [10–12].

## 2. Model description and theoretical approach

### 2.1. Energy level structure

We consider a system of up to three electrons moving in a two-dimensional region bounded by a parabolic potential, with a magnetic field applied perpendicular to the two-dimensional plane, and interacting via a full Coulomb interaction  $V = e^2/\epsilon r_{ij}$ , where  $\epsilon$  is the dielectric constant of the material (typically GaAs, so that  $\epsilon = 12.4$ ), and  $r_{ij}$  is the separation between electrons  $i$  and  $j$ . The Hamiltonian is then given by

$$H = \sum_n \epsilon_n d_n^\dagger d_n + \sum_{nmn'm'} V_{nm}^{n'm'} d_n^\dagger d_m^\dagger d_{n'} d_{m'}, \quad (1)$$

where the single-particle energies  $\epsilon_n$  are connected to the left- and right-circularly polarized oscillator eigenmodes,

$$\epsilon_n = \hbar\Omega_+ \left( N_+ + \frac{1}{2} \right) + \hbar\Omega_- \left( N_- + \frac{1}{2} \right), \quad (2)$$

where  $\Omega_\pm = (\sqrt{4\Omega_0^2 + \omega_c^2} \pm \omega_c)/2$ . Here,  $\Omega_0$  characterizes the parabolic confinement potential typical of quantum dots ( $\propto m\Omega_0^2 r^2$ , with  $\hbar\Omega_0 \approx 1\text{--}2$  meV), and  $\omega_c = eB/mc$  is the cyclotron frequency. We then proceed to separate the Hamiltonian into center-of-mass (CM) coordinates and the remaining relative degrees of freedom. The CM part has a simple harmonic oscillator solution which is independent of the number of electrons, and has a spectrum identical to the single-particle problem—as the interaction only contains relative coordinates. A crucial advantage of the circularly symmetric confinement potential is that the *full* Hamiltonian conserves angular momentum in the direction of the field, so that the Coulomb interaction is ‘block diagonal’, mixing only single-particle states with a given relative angular momentum. Notice that the study and analysis presented in this paper is possible only due to the exact diagonalization of this rather complex quantum mechanical problem. Because of these features, we can confidently explore the fine structure of the level spacing without concerns about the accuracy of the energy level values. Details of the diagonalization process can be found elsewhere [13].

In the analysis that follows, we consider large enough matrix blocks to have several hundred (up to nearly two

thousand) levels where the numerical accuracy exceeds the requirements of the statistical analysis by several orders of magnitude. Notice moreover that the block decimation process used in selecting the corresponding set of eigenvalues also specifies a set of quantum numbers and avoids accidental degeneracies characteristic of mixed sets [6]. Each set studied below corresponds then to only relative-coordinate excitation (as the center of mass has been removed), with a given value of (relative) angular momentum, and even a specific value of total spin. These quantum numbers exhaust the symmetries of the problem and associated conserved quantities [13].

## 2.2. Statistical analysis of level fluctuations

Once a level sequence is selected as described above, we proceed to study the statistical properties of its fluctuation structure. In doing this, it is important to use an *unfolding* procedure, which separates a global variation of the level density from the fluctuation structure of interest [3, 7]. The extraction of the fluctuation spectrum is realized here by a standard process [14]: (a) scaling of the energy eigenvalue sequence  $\{E_i\}$  to cover the interval  $[0,4]$ ; (b) calculation of the 'staircase' function  $N(E)$ , which gives the cumulative number of states below  $E$ , normalized to the total number; and (c) unfolding of the spectrum by defining a new sequence  $x_i = \tilde{N}(E_i)$ , where  $\tilde{N}(E)$  is a smooth polynomial fit to  $N(E)$ .

From this unfolded sequence one can perform a number of statistical analyses. Here, we focus on the nearest-neighbor spacings (NNS), obtained from  $s_j = x_j - x_{j-1}$ , with  $j = 1, \dots, M$ , and the corresponding average  $\langle s \rangle = \sum_j s_j / M$ . Instead of directly showing histograms of the NNS to be compared with the expected limits of Wigner or Poisson probability densities  $P(s)$ , we find that it is preferable to compute the *integrated probability function* [3, 15],

$$I(s) = \int_0^s ds' P(s'). \quad (3)$$

Notice that  $I(s)$  is just the total number of NNS below  $s$ , and it does not depend on the specific binning used, as the histogram representations of  $P(s)$  would.

We will also use below the well-known Brody distribution function  $P_\alpha(s) = (1 + \alpha)\beta_\alpha s^\alpha \exp(-\beta_\alpha s^{\alpha+1})$ , with  $\beta_\alpha = \{\langle s \rangle^{-1} \Gamma[(2 + \alpha)/(1 + \alpha)]\}^{1+\alpha}$ , introduced as a wonderful phenomenological interpolation between various limits of the generic cases [7]. Note that for  $\alpha = 0$ , the Brody function recovers the Poisson distribution,  $P_P(s) = (1/\langle s \rangle) \exp(-s/\langle s \rangle)$ ; while for  $\alpha = 1$  it reduces to the Wigner surmise for the gaussian orthogonal ensemble (GOE) of random matrix theory,  $P_{GOE}(s) = (\pi s/2\langle s \rangle^2) \exp(-\pi s^2/4\langle s \rangle^2)$  [1, 7]. Moreover, and something that proves useful in the analysis of our computed spectra, the corresponding integrated probability function can also be obtained analytically as  $I_\alpha(s) = 1 - \exp(-\beta_\alpha s^{\alpha+1})$ . This allows one to obtain the characteristic  $\alpha$  from a double-log plot, given the relation  $\log \log(1/(1 - I_\alpha)) = \log \beta_\alpha + (\alpha + 1) \log s$  (if indeed one obtains a straight line, as occurs in various systems [14–16]). Many theoretical and experimental systems have been analysed in terms of the Brody function, resulting in intermediate values of  $\alpha$  which change as a characteristic system parameter is varied [1, 3, 7].

From the definition of the integrated probability function  $I(s)$ , it is clear that it asymptotically approaches unity, starting from zero at the origin, and that formally the *slope* of this function is the desired probability density,  $P(s) = dI(s)/ds$ . In fact, the slope near the origin characterizes well the two limiting cases, since as one can see from the Brody form,  $I_\alpha(s \ll \langle s \rangle) \approx \beta_\alpha s^{1+\alpha}$ .

## 3. Results

Figure 1 shows a characteristic staircase function and its corresponding unfolding. (All the results shown in this work correspond to a three-electron system with  $\hbar\Omega_0 = 1$  meV.) Notice that the scaled original spectrum shows a nearly parabolic density of states background, in addition to the stepped fluctuation structure which remains in the unfolded spectrum. We should notice here that the order of the polynomial fit (or even a spline

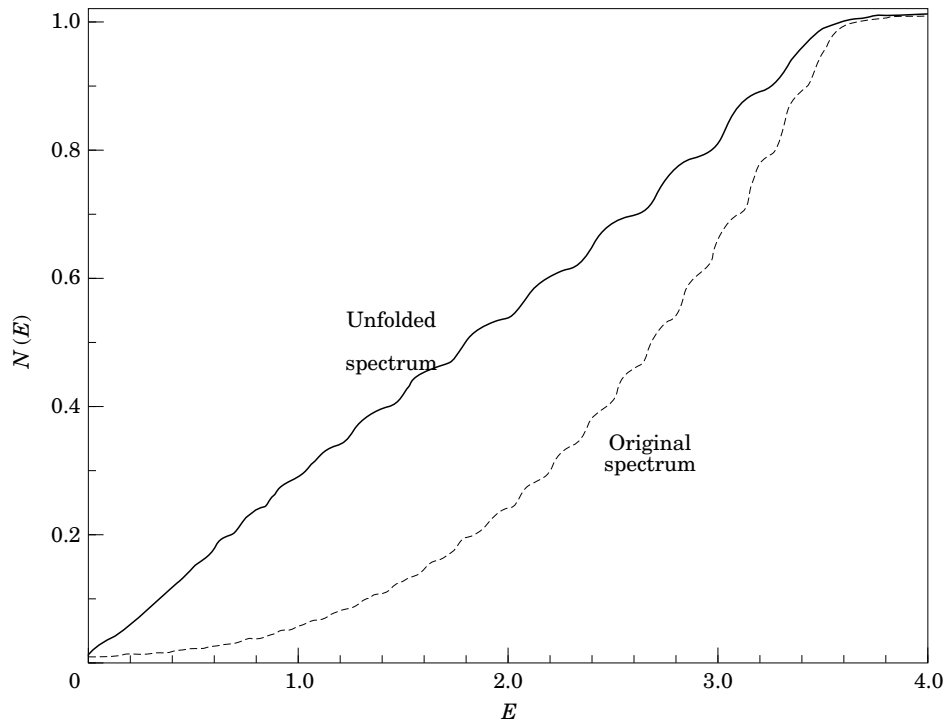


**Fig. 1.** Typical quantum dot level spectrum staircase function. Solid line shows unfolded spectrum, after factorization of smooth background.

fit) does not affect the conclusions below, once the overall smooth dependence has been factored out (here we use a fifth-order polynomial fit, although the higher order coefficients are small). As desired, the unfolded sequence has a linear background, characteristic of a constant density of states [1, 3].

As described in the previous section, we now proceed to calculate the NNS and the corresponding  $I(s)$  function. Fig. 2 shows typical results, here for over 1900 levels with relative angular momentum  $R = 1$  and spin  $S = 1/2$  (both in units of  $\hbar$ ), as well as the corresponding  $I(s)$  curves for the theoretical limits of the Poisson and gaussian ensembles (the latter three distributions have been obtained from integrating the results of random number generators with the appropriate densities  $P(s)$ , to illustrate the robustness of the plots, which exactly agree with the analytical forms given above). It is clear that the  $I(s)$  function generated from the NNS for our two-dimensional quantum dot system does not fall between the Poisson and Wigner traces, as expected for a generic system. In fact, the slope of the  $I(s)$  function for the case shown (corresponding to zero magnetic field) is higher than unity, the Poisson limit. Notice also that despite the steep rise near the origin, the  $I$  function in the quantum dot has a slower asymptotic approach to unity than the Poisson or Wigner traces, indicating a larger probability of finding large values of the NNS (the Poisson curve crosses over at  $s/\langle s \rangle \approx 3.5$ ). This clearly non-generic behavior is the result of the starting point for our calculation, the harmonic ladder [6, 16, 17]. Since the original non-interacting *integrable* level distribution has only zero or one as NNS, an obviously non-Poisson distribution, the electron–electron interaction in the case shown has only begun to break the harmonic ladder, producing the sharply-decreasing probability density shown in Fig. 2.

As the magnetic field increases, for the fixed strength of the electron–electron interaction ‘perturbation’ in

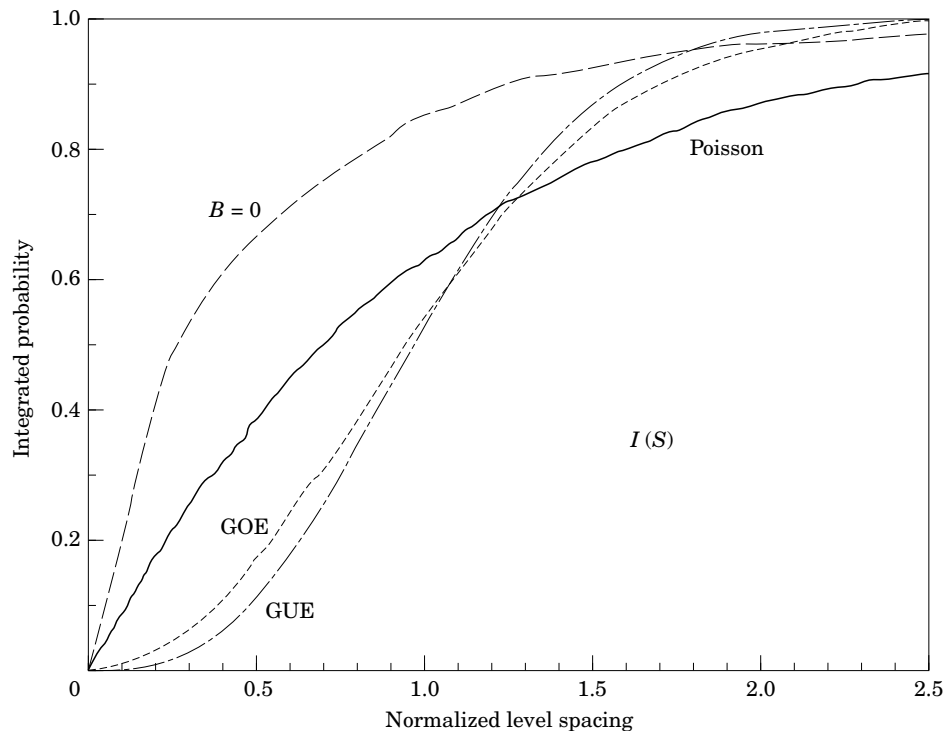


**Fig. 2.** Integrated probability of nearest-neighbor spacings for quantum dot system at  $B = 0$ , with relative angular momentum  $R = \hbar$  and spin  $S = \hbar/2$ . Also shown are limiting cases of Poisson, and gaussian orthogonal (GOE), and unitary (GUE) ensembles.

this problem, the level structure acquires more of a single-particle harmonic character. This behavior, evident in the level structure itself, is to be expected since in the limit of strong magnetic fields one would recover the harmonic-ladder of the Landau levels [18], as the perturbation becomes increasingly weaker in comparison with the kinetic energy quantization. Correspondingly, the distribution function would be expected to evolve towards the peculiar harmonic-oscillator two-step trace as the field increases (see Ref. [6] for a discussion of different harmonic oscillators).

However, the magnetic field dependence is not as monotonic as one would conclude from the previous paragraph. In fact, Fig. 3 shows the corresponding  $I(s)$  traces for different fields, in the case of relative angular momentum  $R = 1$  and total spin  $S = 1/2$ . Here, we see that as the field increases from zero, first the  $I$  function approaches the Poisson trace from above, crosses over to be *under* it for  $B \approx 1$  T, and then moves away again for stronger fields, becoming more and more steep near the origin. Notice also that the  $I(s)$  curve crosses under the Poisson trace at different  $s$  values, depending on the field values.

In other cases, in fact, one can obtain a fit to the Brody function as described above as a double-log plot yields a straight line over most of the range of NNS, and one can reliably assign a value of  $\alpha$ . Figure 4A shows an example of such case with its corresponding  $P(s)$  function (here  $R = 3$ ,  $S = 3/2$ , and  $B = 0$ ), well fitted with a value of  $\alpha = 0.2$ . Notice that the  $P(s)$  function is shown with small bins, to better illustrate its variation, while the  $I(s)$  function shows a much smoother behavior. The solid line through  $P(s)$  is the Brody parametrization with  $\alpha = 0.2$ , while the corresponding fit to the integrated probability  $I(s)$  is basically indistinguishable from the trace shown in the figure. For this value of angular momentum and zero magnetic field, the effect of interactions appears quite important, as it causes a strong departure from the integrable

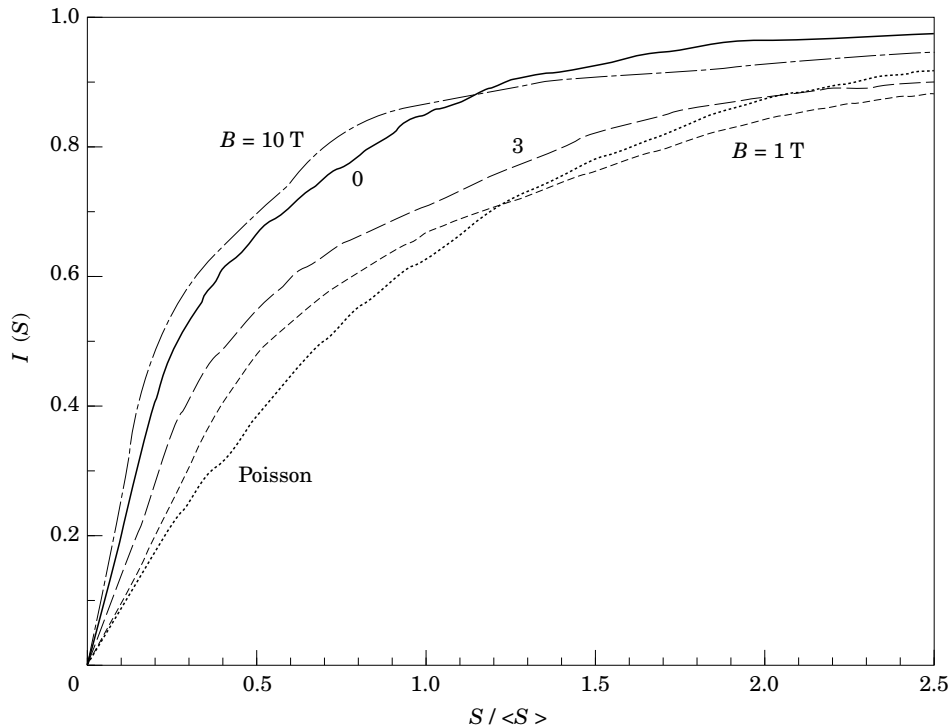


**Fig. 3.** Integrated probability function versus normalized level spacing for quantum dot and different magnetic field values ( $R = \hbar$  and  $S = \hbar/2$ ). Notice non-monotonic field dependence of slope near the origin.

case, and the fluctuations follow a  $P(s)$  which bends downwards for small  $s$  and lies consistently above the Poisson trace for larger  $s$  values. Notice, however, that as the magnetic field increases to  $B = 3$  T, shown in Fig. 4B, the probability density drops faster than the Poisson curve, and the corresponding  $I$  rises sharply near the origin, which cannot be well described by a Brody function [i.e. the double-log plot yields a slope (or  $\alpha$ ) which decreases with increasing  $s$ , indicative of the long tail in the distribution function].

#### 4. Conclusions

We have shown that the level structure in a quantum dot system with interacting electrons via a realistic Coulomb potential exhibits interesting statistical behavior as functions of quantum numbers and applied magnetic fields. In particular, we have found that interactions produce deviations of the non-generic harmonic-oscillator structure, with strong departures from the Poisson or Wigner limits. The details of the observed probability density depend non-monotonically on the magnetic fields, reflecting the effect of the interactions and its competition with the kinetic confinement provided by the applied field.

A number of important questions remain which would allow us to understand the behavior that the study of the fluctuations has uncovered. The connection between different quantum number sets and the effect of interactions is not completely clear, requiring more calculations and a detailed analysis of the quantum number behavior. In particular, the classical system would be expected to have stronger non-integrable behavior as the energy increases, since then the particles can approach each other more, and the corresponding source of non-linearity—the interaction—may play a more important role. How this relates to the given values of the

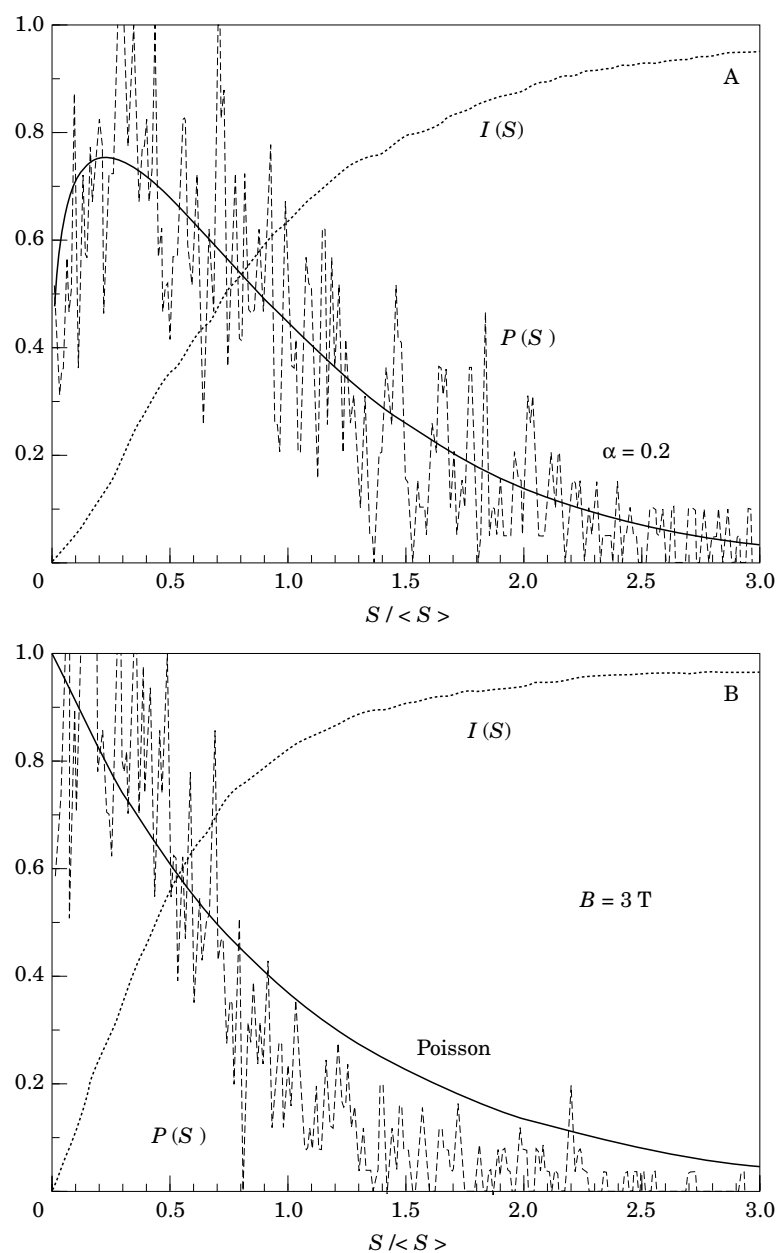


**Fig. 4.** Probability density and its integral for  $R = 3\hbar$  and  $S = 3\hbar/2$ , with (A)  $B = 0$ , and (B)  $B = 3 \text{ T}$ . For zero field, solid line shows fit to Brody function  $P_\alpha(s)$ , with  $\alpha = 0.2$ .

relative angular momentum is at the present not clear (although increasing values of  $R$  would place the system more in the semiclassical limit). The relation between this perturbation via interactions and the analysis of an oscillator system with quartic non-linearities in the Hamiltonian would also be interesting, as the symmetries of both systems are different and the non-linearities relate to different features of the spectra [16, 17].

*Acknowledgements*—This work was supported in part by US-DOE grant No. DE-FG02-91ER45334, the A. v. Humboldt Foundation (SEU), and a grant by the Deutsche Forschungsgemeinschaft (DFG).

### References

- [1] L. E. Reichl, *The Transition to Chaos*, Springer, New York, (1992).
- [2] S. W. McDonald and A. N. Kaufman, *Phys. Rev. Lett.* **42**, 1189 (1979).
- [3] M. C. Gutzwiller, *Chaos in Classical and Quantum Mechanics*, Springer, New York, (1990).
- [4] E. J. Heller, *Phys. Rev. Lett.* **53**, 1515 (1984).
- [5] Z. L. Ji and K. F. Berggren, *Phys. Rev.* **B 52**, 1745 (1995).
- [6] M. V. Berry and M. Tabor, *Proc. Roy. Soc. London A* **356**, 375 (1977).
- [7] T. A. Brody, J. Flores, J. B. French, P. A. Mello, A. Pandey and S. S. M. Wong, *Rev. Mod. Phys.* **53**, 385 (1981).
- [8] A. T. Johnson, L. P. Kouwenhoven, W. de Jong, N. C. van der Vaart, C. J. P. M. Harmans and C. T. Foxon, *Phys. Rev. Lett.* **69**, 1592 (1992); J. Weis, R. Haug, K. v. Klitzing and K. Ploog, *Phys. Rev. Lett.* **71**, 4019 (1993).
- [9] D. Pfannkuche and S. E. Ulloa, *Phys. Rev. Lett.* **74**, 1194 (1995); S. E. Ulloa and D. Pfannkuche, *Superlatt. Microstr.* **15**, 269 (1994); K. Jauregui, W. Häusler, D. Weinmann and B. Kramer, *Phys. Rev.* **B 53**, R1713 (1996).
- [10] L. P. Gorkov and G. M. Eliashberg, *Sov. Phys. JETP* **21**, 940 (1965).
- [11] K. B. Efetov, *Adv. Phys.* **32**, 53 (1983).
- [12] B. L. Altshuler and B. Z. Spivak, *Sov. Phys. JETP* **65**, 343 (1987); B. D. Simons, P. A. Lee and B. L. Altshuler, *Phys. Rev. Lett.* **70**, 4122 (1993).
- [13] D. Pfannkuche, V. Gudmundsson and P. A. Maksym, *Phys. Rev.* **B 47**, 2244 (1993); D. Pfannkuche, and R. R. Gerhardts, *Physica* **189B**, 6 (1993); P. Hawrylak and D. Pfannkuche, *Phys. Rev. Lett.* **70**, 485 (1993).
- [14] T. Terasaka and T. Matsushita, *Phys. Rev.* **B 32**, 538 (1985).
- [15] R. Badrinarayanan, J. V. Jose and G. Chu, *Physica* **83D**, 1 (1995).
- [16] E. Haller, H. Köppel and L. S. Cederbaum, *Phys. Rev. Lett.* **52**, 1665 (1984).
- [17] Y. H. Zheng and R. A. Serota, *Phys. Rev.* **B 50**, 2492 (1994).
- [18] U. Merkt, J. Huser and M. Wagner, *Phys. Rev.* **B 43**, 7320 (1991); P. A. Maksym and T. Chakraborty, *Phys. Rev. Lett.* **65**, 108 (1990).